

A model of in vitro UDP-glucuronosyltransferase inhibition by bile acids predicts possible metabolic disorders[§]

Zhong-Ze Fang,^{1,*†,§} Rong-Rong He,^{1,**} Yun-Feng Cao,[†] Naoki Tanaka,[§] Changtao Jiang,[§] Kristopher W. Krausz,[§] Yunpeng Qi,[§] Pei-Pei Dong,^{††} Chun-Zhi Ai,[†] Xiao-Yu Sun,[†] Mo Hong,[†] Guang-Bo Ge,[†] Frank J. Gonzalez,[§] Xiao-Chi Ma,^{2,§§} and Hong-Zhi Sun^{2,*}

First Affiliated Hospital of Liaoning Medical University,* Jinzhou 121001, China; Joint Center for Translational Medicine,[†] Dalian Institute of Chemical Physics Chinese Academy of Sciences and First Affiliated Hospital of Liaoning Medical University, Dalian 116023, China; Laboratory of Metabolism,[§] Center for Cancer Research, National Cancer Institute, Bethesda, MD 20892; Pharmacy College,** Jinan University, Guangzhou 510632, China; and Academy of Integrative Medicine^{††} and College of Pharmacy, Pharmacokinetic and Drug Transport Key Laboratory,^{§§} Dalian Medical University, Dalian 116044, China

Abstract Increased levels of bile acids (BAs) due to the various hepatic diseases could interfere with the metabolism of xenobiotics, such as drugs, and endobiotics including steroid hormones. UDP-glucuronosyltransferases (UGTs) are involved in the conjugation and elimination of many xenobiotics and endogenous compounds. The present study sought to investigate the potential for inhibition of UGT enzymes by BAs. The results showed that tauroolithocholic acid (TLCA) exhibited the strongest inhibition toward UGTs, followed by lithocholic acid. Structure-UGT inhibition relationships of BAs were examined and in vitro-in vivo extrapolation performed by using in vitro inhibition kinetic parameters (K_i) in combination with calculated in vivo levels of TLCA. Substitution of a hydrogen with a hydroxyl group in the R1, R3, R4, R5 sites of BAs significantly weakens their inhibition ability toward most UGTs. The in vivo inhibition by TLCA toward UGT forms was determined with following orders of potency: UGT1A4 > UGT2B7 > UGT1A3 > UGT1A1 ~ UGT1A7 ~ UGT1A10 ~ UGT2B15. **In conclusion,** these studies suggest that disrupted homeostasis of BAs, notably tauroolithocholic acid, found in various diseases such as cholestasis, could lead to altered metabolism of xenobiotics and endobiotics through inhibition of UGT enzymes.—Fang, Z-Z., R-R. He, Y-F. Cao, N. Tanaka, C. Jiang, K. W. Krausz, Y. Qi, P-P. Dong, C-Z. Ai, X-Y. Sun, M. Hong, G-B. Ge, F. J. Gonzalez, X-C. Ma, and H-Z. Sun. **A model of in vitro UDP-glucuronosyltransferase inhibition by bile acids predicts possible metabolic disorders.** *J. Lipid Res.* 2013. 54: 3334–3344.

Supplementary key words cholestasis • endobiotics • structure-UDP-glucuronosyltransferase inhibition relationship • xenobiotics

Bile acids (BAs), the major end-products of cholesterol metabolism, play a key role in the solubilization, absorption, and transportation of dietary lipids in the intestine (1). In humans, the most abundant BAs contain cholic acid (CA), chenodeoxycholic acid, deoxycholic acid, lithocholic acid (LCA), and ursodeoxycholic acid (UDCA) (2). In the livers of mice and rats, chenodeoxycholic acid can be further converted into α - and β -muricholic acid (3). Under normal conditions, BAs exist at low concentrations in the peripheral circulation. Various hepatic and intestinal diseases can significantly affect the total BA levels and disrupt the BA homeostasis. For example, cholestasis can disturb the bile secretory process, leading to the accumulation of toxic BAs in the liver (4).

Abbreviations: AUC, area under the curve; AZT, azidothymidine; BA, bile acid; CA, cholic acid; CDCA, sodium chenodeoxycholate; DCA, sodium deoxycholate; DHCA, dehydrocholic acid; FXR, farnesoid X receptor; GCA, glycocholic acid hydrate; HDCA, hyodeoxycholic acid; HLM, human liver microsome; I.D., inner diameter; LCA, lithocholic acid; 4-MU, 4-methylumbelliferone; 4-MUG, 4-methylumbelliferone- β -D-glucuronide; PPAR, peroxisome proliferator-activated receptor; TCDCa, taurochenodeoxycholate; TDCA, sodium taurodeoxycholate hydrate; TFP, trifluoperazine; TLCA, tauroolithocholic acid; TUDCA, sodium tauroursodeoxycholate; UDCA, ursodeoxycholic acid; UDPGA, uridine-5'-diphosphoglucuronic acid trisodium salt; UGT, UDP-glucuronosyltransferase; .

¹Z-Z. Fang and R-R. He contributed equally to this work.

²To whom correspondence should be addressed.

e-mail: cmushz@163.com (X-Y.S.); maxc1978@163.com (X-C.M)

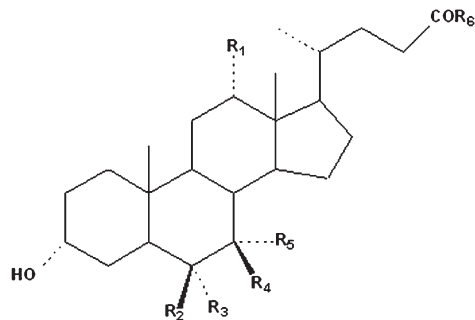
[§]The online version of this article (available at <http://www.jlr.org>) contains supplementary data in the form of three figures and one table.

This work was supported by the National Natural Science Foundation of China (No. 81202586, 81274047 and No. 81102507) and the National Cancer Institute, Center for Cancer Research, Intramural Research Program. The authors have declared no conflicts of interest.

Manuscript received 30 May 2013 and in revised form 27 September 2013.

Published, JLR Papers in Press, October 10, 2013

DOI 10.1194/jlr.M040519



Bile acids	R1	R2	R3	R4	R5
HDCA	H	H	OH	H	H
LCA	H	H	H	H	H
CDCA	H	H	H	H	OH
UDCA	H	H	H	OH	H
CA	OH	H	H	H	OH
DCA	OH	H	H	H	H

Bile acids	R6
unconjugate	OH
Taurine conjugate	NH(CH ₂) ₂ SO ₃ H
Glycine conjugate	NHCH ₂ COOH

Fig. 1. The structure of BAs used in this study.

Human UDP-glucuronosyltransferases (UGTs), endogenous membrane proteins located in endoplasmic reticulum, can conjugate various endogenous and exogenous compounds (5). BAs are substrates of UGTs, and UGT-catalyzed glucuronidation of BAs facilitate their hydrophilicity, increase their elimination from the liver, and decrease their potential for hepatic toxicity (6–8). For example, UGT1A3 can catalyze C24-glucuronidation of chenodeoxycholic acid, LCA, and hyodeoxycholic acid (HDCA) through forming acyl glucuronides (9). UGT2B4 is involved in the 6 α -glucuronidation of BAs such as HDCA (10). UGT2B7 is the UGT isoform involved in the 3 α - and 6 α -glucuronidation of primary, secondary, and hydroxylated BA (9).

As substrates for UGT enzymes, BAs might also exhibit inhibitory effects toward various UGT forms. Previous studies revealed that some BA components exhibit inhibitory effects toward 4-methylumbelliferone (4-MU) glucuronidation, including LCA, dehydrocholic acid (DHCA), and sodium chenodeoxycholate (CDCA) (11). However, the complete inhibition profile of BAs toward different UGT forms remains unclear. Additionally, the BA structure-UGT inhibition relationships are important to determine what structural basis of BAs affects their inhibition potentials toward different UGTs. Therefore, the present study evaluated the inhibition capability of various BAs toward UGT forms in liver and intestine. As previously described (12), recombinant UGT isoform-catalyzed 4-MU glucuronidation reactions were used to evaluate the inhibition potential of BAs toward UGTs except for UGT1A4, and where trifluoperazine (TFP) glucuronidation was performed as the standard reaction to evaluate the inhibition potential of BAs toward UGT1A4 activity.

TABLE 1. Initial screening of BAs (100 μ M) toward various important UGT forms

Bile Acids	UGT1A1	UGT1A3	UGT1A4	UGT1A6	UGT1A7	UGT1A8	UGT1A9	UGT1A10	UGT2B7	UGT2B15
HDCA	44.6 \pm 0.4***	26.1 \pm 6.8*	13.7 \pm 0.5**	95.4 \pm 2.1	47.8 \pm 0.5***	84.0 \pm 6.1*	50.4 \pm 4.3*	52.5 \pm 0.9***	9.5 \pm 2.0**	34.6 \pm 0.4***
LCA	21.1 \pm 8.0***	16.4 \pm 0.5*	0.0 \pm 0.0***	19.9 \pm 1.3**	30.0 \pm 2.2***	64.3 \pm 7.1**	65.2 \pm 17.4	25.0 \pm 0.3***	15.7 \pm 1.9**	0.3 \pm 0.0***
TCDCa	17.5 \pm 6.7***	21.6 \pm 1.3*	27.8 \pm 2.1**	84.6 \pm 1.6*	52.7 \pm 3.3***	59.1 \pm 20.0*	75.3 \pm 1.1*	41.0 \pm 8.2**	28.1 \pm 2.0**	28.4 \pm 1.1***
Taurocholic acid sodium salt hydrate	62.7 \pm 6.1**	66.7 \pm 17.3	73.8 \pm 1.4	105.8 \pm 0.4	94.1 \pm 2.5	75.5 \pm 8.1*	94.7 \pm 6.2	71.9 \pm 0.3**	69.3 \pm 7.7*	70.2 \pm 3.9*
CDCA	37.7 \pm 8.4**	47.2 \pm 8.0	20.2 \pm 1.4**	92.9 \pm 2.6	47.4 \pm 12.7**	29.2 \pm 3.1***	74.0 \pm 1.2*	39.9 \pm 2.3***	15.4 \pm 2.1**	19.8 \pm 1.0***
TLCA	5.4 \pm 0.0***	3.4 \pm 0.4*	0.0 \pm 0.0***	52.4 \pm 0.2**	9.1 \pm 8.8***	24.1 \pm 3.5***	54.4 \pm 7.1*	14.8 \pm 6.8***	1.7 \pm 0.6**	5.3 \pm 0.0***
UDCA	27.4 \pm 0.4*	92.8 \pm 49.8	25.3 \pm 0.8**	85.0 \pm 0.9*	45.7 \pm 9.6**	29.8 \pm 3.8***	54.5 \pm 5.8*	57.6 \pm 1.4***	46.2 \pm 4.9*	54.1 \pm 1.2**
CA	61.9 \pm 0.9**	135.5 \pm 18.8	73.0 \pm 1.1	100.7 \pm 1.0	103.4 \pm 2.8	86.1 \pm 3.2*	89.0 \pm 3.7	74.4 \pm 0.5**	83.2 \pm 7.9	72.1 \pm 0.2**
DHCA	76.4 \pm 13.3	117.5 \pm 30.2	80.7 \pm 25.3	95.0 \pm 0.7	80.9 \pm 1.7**	87.1 \pm 16.0	83.0 \pm 3.5	90.5 \pm 2.9*	81.0 \pm 3.1	77.7 \pm 1.1*
DCA	33.9 \pm 2.3***	57.8 \pm 11.8	43.8 \pm 21.8*	90.3 \pm 2.5	68.0 \pm 3.7**	88.7 \pm 32.5	67.5 \pm 2.6*	39.1 \pm 1.5***	45.8 \pm 2.2*	35.4 \pm 1.0***
TUDCA	10.6 \pm 0.1***	49.1 \pm 8.5	30.8 \pm 4.6**	76.9 \pm 2.4*	48.8 \pm 11.1**	59.3 \pm 0.6***	82.9 \pm 9.1	38.2 \pm 13.2**	26.1 \pm 2.3**	25.3 \pm 0.7***
TDCA	34.1 \pm 0.1**	61.1 \pm 8.8	41.1 \pm 13.3	93.4 \pm 1.1	60.4 \pm 2.5***	74.7 \pm 11.3	85.0 \pm 0.5	50.8 \pm 1.0*	33.4 \pm 2.0*	40.7 \pm 1.9***
GCA	65.4 \pm 4.5**	143.2 \pm 44.3	54.5 \pm 10.3	91.6 \pm 2.9	82.0 \pm 15.0	80.9 \pm 8.7	94.0 \pm 4.8	75.7 \pm 3.8**	48.4 \pm 3.5*	63.4 \pm 1.5**

The values shown are the residual activity, which was calculated using the following equation: % residual activity = (the activity at 100 μ M BAs/the control activity at 0 μ M BAs) \times 100%. * P < 0.05, ** P < 0.01, *** P < 0.001, compared with control activity.

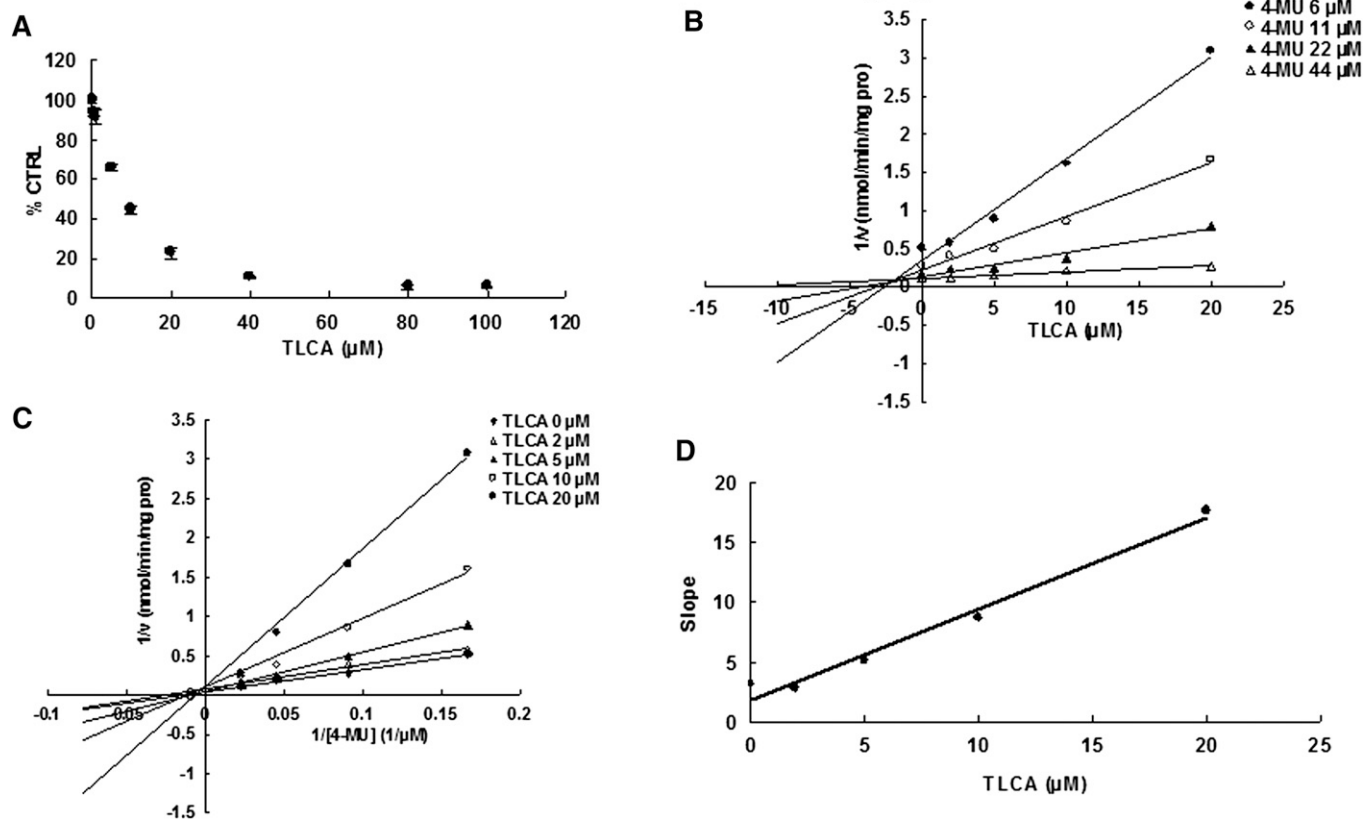
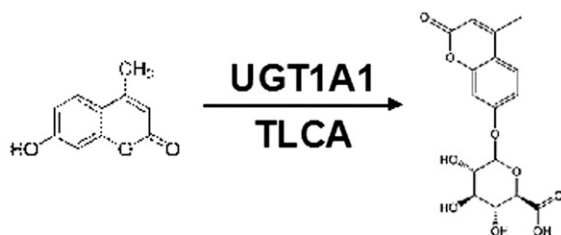


Fig. 2. Evaluation of TLCA's inhibition toward recombinant UGT1A1-catalyzed 4-MU glucuronidation. **A:** TLCA exhibited concentration-dependent inhibition toward recombinant UGT1A1-catalyzed 4-MU glucuronidation. **B:** Dixon plot of TLCA's inhibition toward recombinant UGT1A1-catalyzed 4-MU glucuronidation. **C:** Lineweaver-Burk plot of TLCA's inhibition toward recombinant UGT1A1-catalyzed 4-MU glucuronidation. **D:** Second plot of TLCA's inhibition toward recombinant UGT1A1-catalyzed 4-MU glucuronidation. The data point represents the mean of the duplicate experiments.

MATERIALS AND METHODS

Materials

4-MU, 4-methylumbelliferone- β -D-glucuronide (4-MUG), Tris-HCl, 7-hydroxycoumarin, azidothymidine (AZT) (purity $\geq 98\%$), TFP (purity $\geq 99\%$), estradiol (purity $\geq 98\%$), and uridine-5'-diphosphoglucuronic acid trisodium salt (UDPGA) were purchased from Sigma-Aldrich (St. Louis, MO). Recombinant human UGT isoforms (UGT1A1, UGT1A3, UGT1A4, UGT1A6, UGT1A7, UGT1A8, UGT1A9, UGT1A10, UGT2B7, and UGT2B15) expressed in baculovirus-infected insect cells were obtained from BD Gentest Corp. (Woburn, MA). HDCA, LCA, sodium taurochenodeoxycholate (TCDC), taurocholic acid sodium salt hydrate, CDCA, tauro lithocholic acid (TLCA), UDCA, CA, DHCA, sodium deoxycholate (DCA), sodium tauroursodeoxycholate (TUDCA), sodium taurodeoxycholate hydrate (TDCA), and glycocholic acid hydrate (GCA) were obtained from Sigma-Aldrich. The purity of these compounds was above 95%. All other reagents were of HPLC grade or of the highest grade commercially available.

Initial screening of BAs' inhibition toward the activity of recombinant UGTs

The inhibition capability of BAs toward all the UGT forms, except UGT1A4, was evaluated using recombinant UGT-catalyzed 4-MU glucuronidation as the probe reaction, as previously described (12, 13). The incubation system (total volume 200 μ l) contained recombinant UGTs, 5 mM UDPGA, 5 mM MgCl₂, 50 mM Tris-HCl (pH 7.4), and 4-MU in the absence or presence of different concentrations of various BAs. The incubation time used and protein concentration were previously determined to ensure the reaction rate within the linear range. The 4-MU concentration was equal to known K_m or S_{50} values for each UGT form. The concentrations of 4-MU and recombinant UGTs, and incubation time are given in supplementary Table I. The incubation reaction was initiated through addition of UDPGA to the mixture after a 5 min preincubation at 37°C. The reactions were quenched by adding 100 μ l acetonitrile with 7-hydroxycoumarin (100 μ M) as internal standard. The mixture was centrifuged at 20,000 g for 10 min, and an aliquot of supernatant was transferred to an auto-injector vial for HPLC analysis. The HPLC

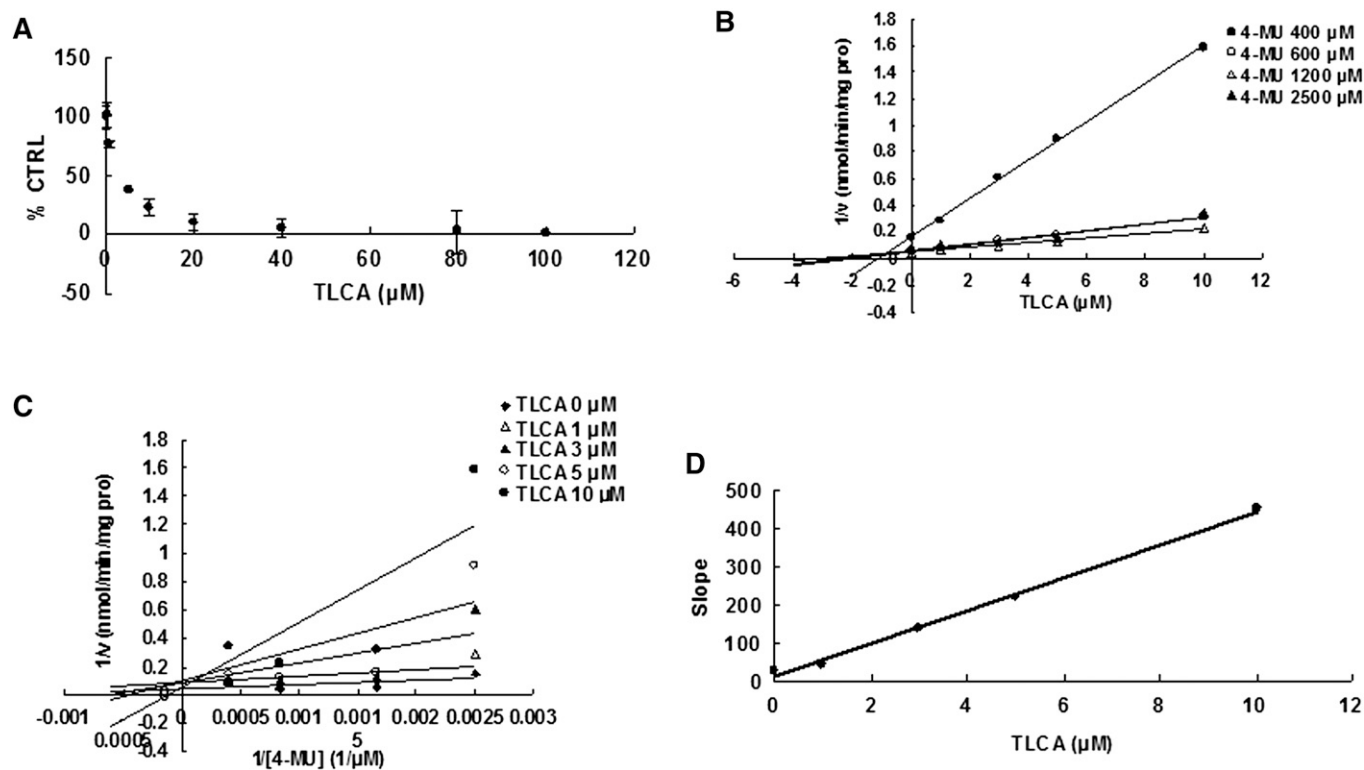
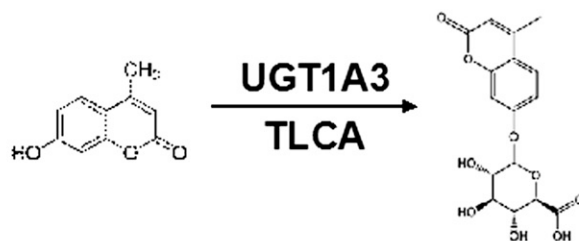


Fig. 3. Evaluation of TLCA's inhibition toward recombinant UGT1A3-catalyzed 4-MU glucuronidation. **A:** TLCA exhibited concentration-dependent inhibition toward recombinant UGT1A3-catalyzed 4-MU glucuronidation. **B:** Dixon plot of TLCA's inhibition toward recombinant UGT1A3-catalyzed 4-MU glucuronidation. **C:** Lineweaver-Burk plot of TLCA's inhibition toward recombinant UGT1A3-catalyzed 4-MU glucuronidation. **D:** Second plot of TLCA's inhibition toward recombinant UGT1A3-catalyzed 4-MU glucuronidation. The data point represents the mean of the duplicate experiments.

system (Shimadzu, Kyoto, Japan) contained a SCL-10A system controller, two LC-10AT pumps, a SIL-10A auto-injector, and a SPD-10AVP UV detector. Chromatographic separation was carried out using a C18 column (4.6 × 200 mm, 5 μm, Kromasil) at a flow rate of 1 ml/min and UV detector at 316 nm. The mobile phase consisted of acetonitrile (A) and water containing 0.5% (v/v) formic acid (B). The following gradient condition was used: 0–15 min, 95–40% B; 15–20 min, 10% B; 20–30 min, 95% B. The calculation curve was generated by peak area ratio (4-MUG/internal standard) over the concentration range of 4-MUG 0.1–100 mM. The curve was linear over this concentration range, with an r^2 value >0.99. The limits of detection and quantification were determined at signal-to-noise ratios of 3 and 10, respectively. The accuracy and precision for each concentration was more than 95%.

Due to the low catalytic activity of UGT1A4 toward 4-MU glucuronidation, the UGT1A4-catalyzed TFP glucuronidation was performed to evaluate the inhibition potential of BAs toward UGT1A4 activity. TFP (40 μM, near its K_m value), was incubated with recombinant UGT1A4 (0.1 mg/ml) at 37°C for 20 min in the absence or presence of BAs (14).

TLCA's inhibition toward hepatocyte UGT-catalyzed 4-MU glucuronidation

Primary hepatocytes were isolated from C57BL/6NCr mice and cultured as previously described (15). 4-MU (50 μM) and TLCA (50 nM) were added to the medium. After a 1 h incubation at 37°C, the medium and cells were isolated. Methanol (v/v) 1:1 and 5 μM chlorpropamide as an internal standard were added to the medium, and 1 ml methanol with 5 μM chlorpropamide as an internal standard were added to extract the compounds in the cells. After centrifugation at 20,000 g for 10 min, the aliquot of supernatant was determined to detect the formation of 4-MUG.

BAs' inhibition toward human liver microsomes-catalyzed azidothymidine and estradiol glucuronidation

Twenty-five donor pooled human liver microsomes (HLMs) were purchased from Research Institute for Liver Diseases (RILD, Shang Hai, China). For azidothymidine (AZT) glucuronidation, the typical incubation system (total volume 200 μl) contained 0.5 mg/ml HLMs, 5 mM UDPGA, 5 mM $MgCl_2$, 50 mM Tris-HCl (pH 7.4), 50 μg/mg protein alamethicin, and AZT (concentration

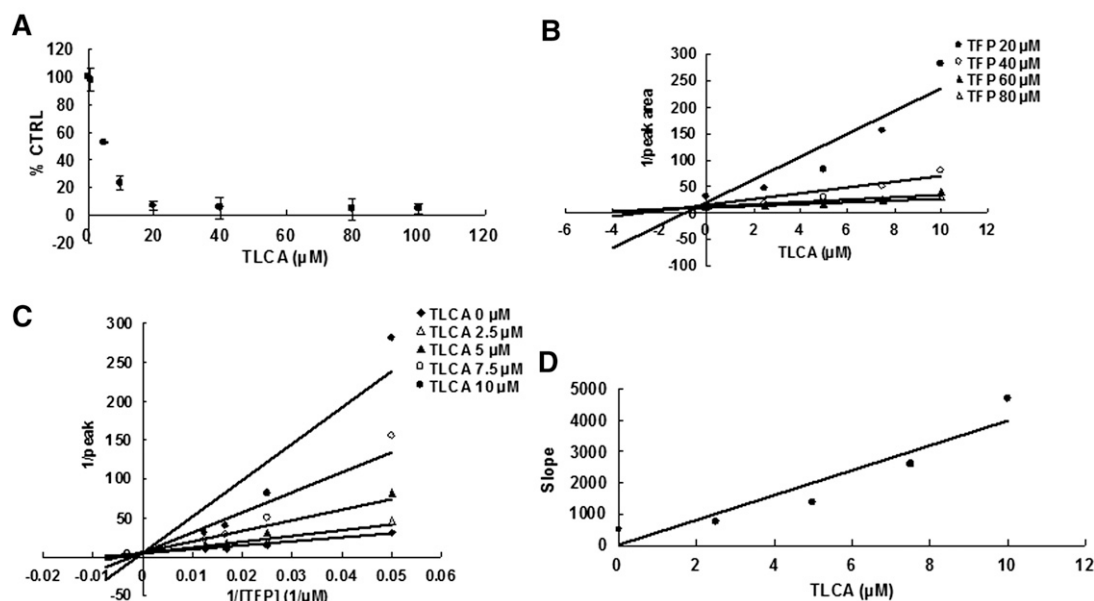
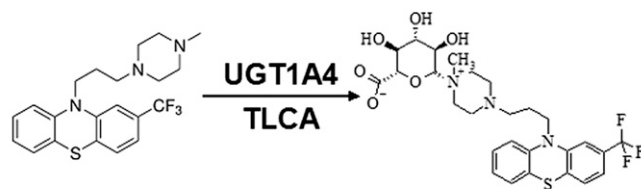


Fig. 4. Evaluation of TLCA's inhibition toward recombinant UGT1A4-catalyzed TFP glucuronidation. A: TLCA exhibited concentration-dependent inhibition toward recombinant UGT1A4-catalyzed TFP glucuronidation. B: Dixon plot of TLCA's inhibition toward recombinant UGT1A4-catalyzed TFP glucuronidation. C: Lineweaver-Burk plot of TLCA's inhibition toward recombinant UGT1A4-catalyzed TFP glucuronidation. D: Second plot of TLCA's inhibition toward recombinant UGT1A4-catalyzed TFP glucuronidation. The data point represents the mean of the duplicate experiments.

is corresponding to the K_m value). The incubation time was 30 min. After centrifugation at 20,000 *g* for 10 min, aliquots of the supernatants were analyzed by HPLC (Shimadzu, Kyoto, Japan), equipped with a SCL-10A system controller, two LC-10AT pumps, a SIL-10A auto sampler, and a SPD-10AVP UV detector. A C-18 column (250 mm \times 4.6 mm I.D., 5 μ m, Kromasil) was used to separate AZT and its glucuronide. The mobile phase was acetonitrile (A) and 0.2% formic acid (B) at a flow rate of 1.0 ml/min, with an isocratic: 0–25 min 90% B. The detector wavelength was set at 260 nm. Because there was no standard for the AZT glucuronide, a standard curve of AZT was used to quantify glucuronide formation.

Estradiol (10 μ M) was incubated with HLMs for 20 min, with the final protein concentrations of 0.25 mg/ml. Estradiol glucuronidation samples were analyzed on the Ultra Fast Liquid Chromatography (UFLC) system. A Shim-pack XR-ODS (50.0 mm \times 2.0 mm I.D., 2.2 μ m, Shimadzu) analytical column with an ODS guard column (5 mm \times 2.0 mm I.D., 2.2 μ m, Shimadzu) was used and kept at 40°C. The mobile phase consisted of acetonitrile (A) and 0.2% formic acid (B) at a flow rate of 0.3 ml/min, with a gradient: 0–9 min, 90% B–30% B; 9–12.5 min, 5% B; 12.5–16 min, balance to 90% B. The detector wavelength was set at 250 nm. A standard curve of the estradiol-3-O-glucuronide was used to quantify glucuronide formation.

In vitro-in vivo extrapolation

The reaction velocity was determined at different concentrations of substrates and inhibitors. The durations in the inhibition

kinetic study were the same as the initial screening study. Dixon and Lineweaver-Burk plots were used for determination of inhibition kinetic type. The second plot of slopes from the Lineweaver-Burk plot versus inhibitor concentrations was used to calculate the K_i value. The in vivo inhibition magnitude is affected by both in vitro inhibition kinetic parameters (K_i) and in vivo concentrations of inhibitors. Therefore, the following equation was employed to predict in vivo situation.

$$AUC_i/AUC = 1 + [I]_{in\ vivo}/K_i$$

The terms are defined as follows: AUC_i/AUC is the predicted ratio of in vivo exposure of xenobiotics or endogenous compounds in control and disease situations, K_i is the reversible inhibition constant, and $[I]_{in\ vivo}$ is the in vivo concentration of BAs.

RESULTS

Structure-inhibition relationship of BAs toward UGT isoforms

The structures of tested BAs are listed in **Fig. 1**, and the inhibitory capabilities of these BAs toward different UGT forms is given in **Table 1**. Among the tested UGT enzymes, the activity of UGT1A6, UGT1A8, and UGT1A9 were not affected by various BAs. Among the tested BAs at 100 μ M, TCDCa, taurocholic acid sodium salt hydrate, CDCA, UDCA, CA, DHCA, DCA, TUDCA, TDCA, and GCA exhibited

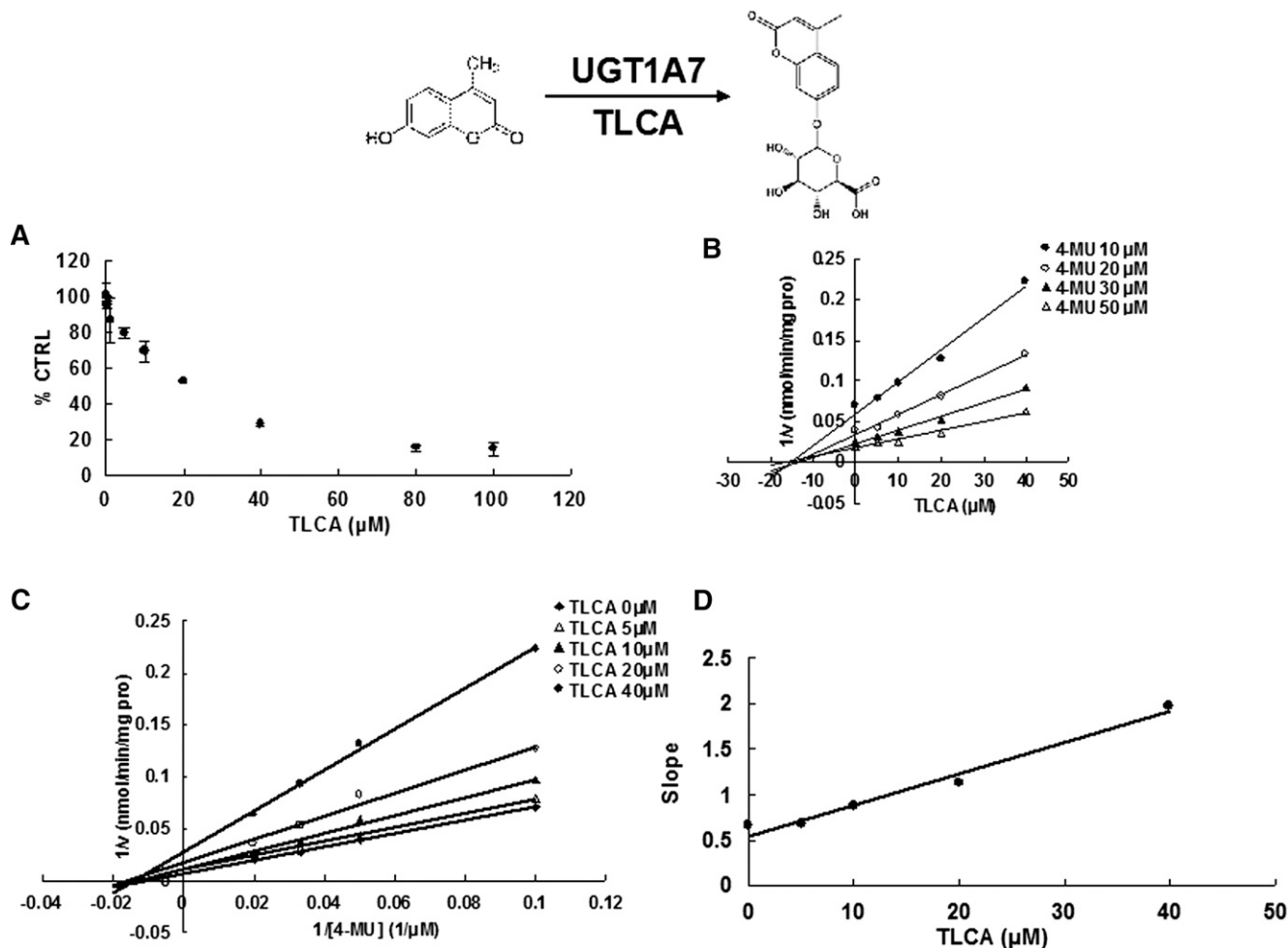


Fig. 5. Evaluation of TLCA's inhibition toward recombinant UGT1A7-catalyzed 4-MU glucuronidation. A: TLCA exhibited concentration-dependent inhibition toward recombinant UGT1A7-catalyzed 4-MU glucuronidation. B: Dixon plot of TLCA's inhibition toward recombinant UGT1A7-catalyzed 4-MU glucuronidation. C: Lineweaver-Burk plot of TLCA's inhibition toward recombinant UGT1A7-catalyzed 4-MU glucuronidation. D: Second plot of TLCA's inhibition toward recombinant UGT1A7-catalyzed 4-MU glucuronidation. The data point represents the mean of the duplicate experiments.

no or weak inhibition toward all the tested UGT forms, with inhibition magnitudes less than 90%. HDCA exerted 90.5% inhibition toward UGT2B7-catalyzed 4-MU glucuronidation, and low inhibition toward other UGTs. LCA exhibited the strongest inhibition (more than 90%) toward UGT1A4 and UGT2B15. TLCA showed strong inhibition toward most of UGT forms, including UGT1A1 (94.6%), UGT1A3 (96.6%), UGT1A4 (100%), UGT1A7 (90.9%), UGT2B7 (98.3%), and UGT2B15 (94.7%).

The structure-UGT inhibition relationship can be observed using the combination of the BAs' structures (Fig. 1) and the UGT inhibition results (Table 1). The substitution of hydrogen with hydroxyl group at the R₁, R₃, R₄, R₅ sites significantly weakens the inhibition toward most UGT forms. In comparison with the inhibition magnitude of LCA and TLCA toward UGT2B7, a conclusion can be drawn that the taurine conjugation of LCA can strengthen the inhibition potential toward UGT2B7.

To demonstrate the physiological significance of these observations, TLCA (50 nM) was added to the medium to investigate whether it could inhibit hepatocyte UGT-catalyzed

4-MU glucuronidation activity. The results showed significant inhibition of TLCA toward hepatocyte UGT-catalyzed 4-MU glucuronidation (supplementary Fig. I).

Different inhibition type and kinetic parameters of TLCA toward UGT forms

Due to the potent inhibition of TLCA toward many UGT forms, the inhibition kinetic type and parameters (K_i) were further investigated. Both Dixon and Lineweaver-Burk plots were employed to evaluate the inhibition type, and the second plot using the slopes obtained from Lineweaver-Burk plot versus the concentrations of TLCA was used to calculate the inhibition kinetic parameters (K_i). If the intersection point was located in the vertical axis and the second quadrant in the Lineweaver-Burk plot and Dixon plot respectively, the inhibition type was classified as competitive inhibition. If the intersection point was located in horizontal axis in both Dixon and Lineweaver-Burk plots, the inhibition type was classified as noncompetitive inhibition. The results show that TLCA competitively inhibited UGT1A1 (Fig. 2B, C),

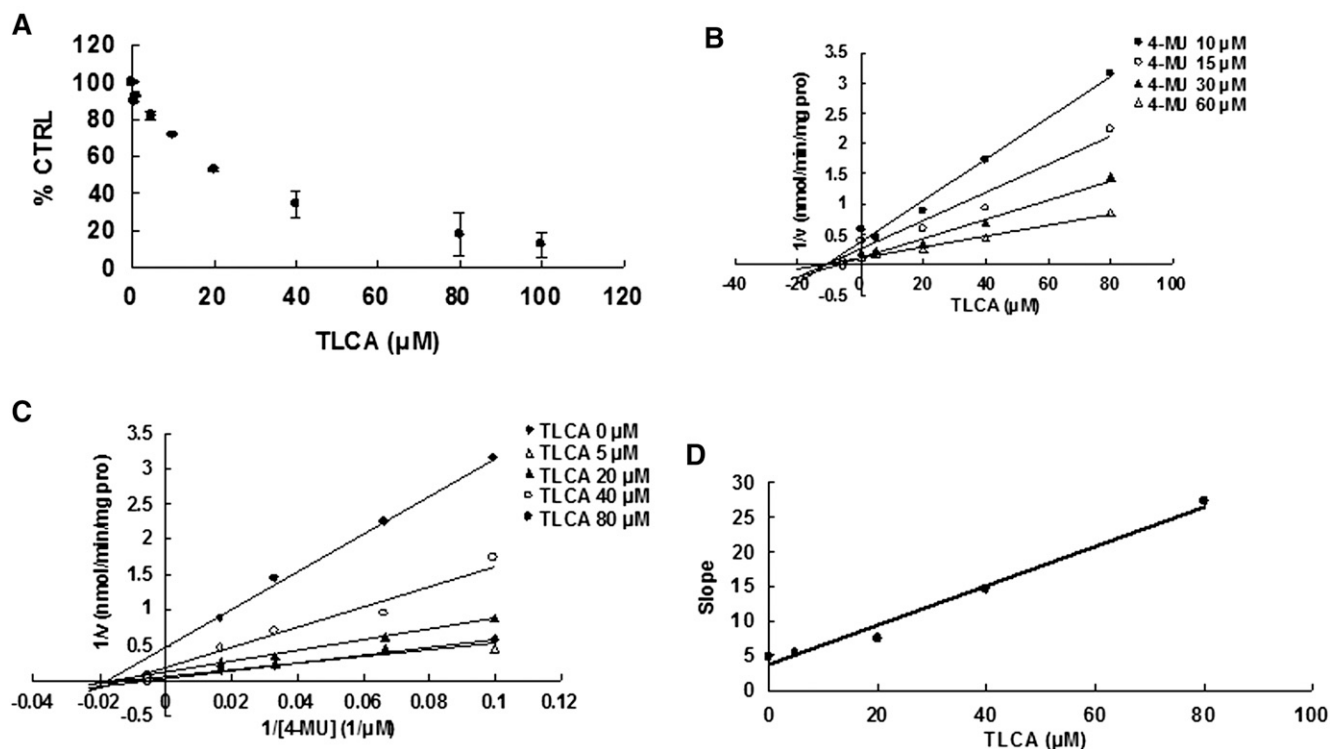
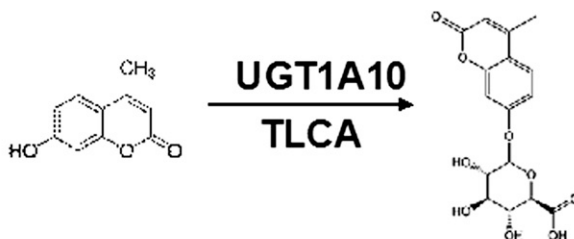


Fig. 6. Evaluation of TLCA's inhibition toward recombinant UGT1A10-catalyzed 4-MU glucuronidation. **A:** TLCA exhibited concentration-dependent inhibition toward recombinant UGT1A10-catalyzed 4-MU glucuronidation. **B:** Dixon plot of TLCA's inhibition toward recombinant UGT1A10-catalyzed 4-MU glucuronidation. **C:** Lineweaver-Burk plot of TLCA's inhibition toward recombinant UGT1A10-catalyzed 4-MU glucuronidation. **D:** Second plot of TLCA's inhibition toward recombinant UGT1A10-catalyzed 4-MU glucuronidation. The data point represents the mean of the duplicate experiments.

UGT1A3 (Fig. 3B, C), UGT1A4 (Fig. 4B, C), and noncompetitively inhibited UGT1A7 (Fig. 5B, C) and UGT1A10 (Fig. 6B, C). The inhibition of UGT2B7 (Fig. 7B, C) and UGT2B15 (Fig. 8B, C) was also best fit to competitive inhibition. The inhibition kinetic parameters (K_i) were calculated to be 2.4, 0.3, 0.03, 16.0, 12.9, 0.1, and 3.3 μM for the activity of UGT1A1 (Fig. 2D), UGT1A3 (Fig. 3D), UGT1A4 (Fig. 4D), UGT1A7 (Fig. 5D), UGT1A10 (Fig. 6D), UGT2B7 (Fig. 7D), and UGT2B15 (Fig. 8D), respectively.

Two typical substrates, AZT and estradiol, were then selected as representative of xenobiotic and endogenous substrates to clarify the influence of TLCA toward the glucuronidation of these two compounds. The concentration-dependent inhibition of TLCA toward the glucuronidation of AZT and estradiol was also demonstrated (supplementary Fig. IIA, Fig. 3A). Furthermore, the competitive inhibition of TLCA toward the glucuronidation of AZT (supplementary Fig. IIB, C) and estradiol (supplementary Fig. IIIB, C) was demonstrated. The inhibition kinetic parameters (K_i) were calculated to be 0.3 and 2.2 μM

for inhibition of TLCA toward AZT and estradiol glucuronidation (supplementary Figs. IID, IIID).

Prediction of in vivo metabolic disorders in humans

Due to the strongest inhibition potential of TLCA toward different UGT enzymes, changes in in vivo metabolism could be predicted based on the concentration of TLCA. The concentration of TLCA in serum obtained from mice with intrahepatic cholestasis of pregnancy was reported to be 0.3 μM (16). Using this concentration in combination with the K_i values for the inhibition of TLCA toward 4-MU glucuronidation, the AUC_i/AUC values were calculated to be 1.1, 2, 11, 1.02, 1.02, 4, and 1.1 for UGT1A1, UGT1A3, UGT1A4, UGT1A7, UGT1A10, UGT2B7, and UGT2B15, respectively. In humans, the TLCA concentration was reported to never exceed 25 nM (17). Using this maximum value, the AUC_i/AUC values were calculated to be 1.01, 1.08, 1.83, 1.002, 1.002, 1.25, and 1.008 for UGT1A1, UGT1A3, UGT1A4, UGT1A7, UGT1A10, UGT2B7, and UGT2B15, respectively.

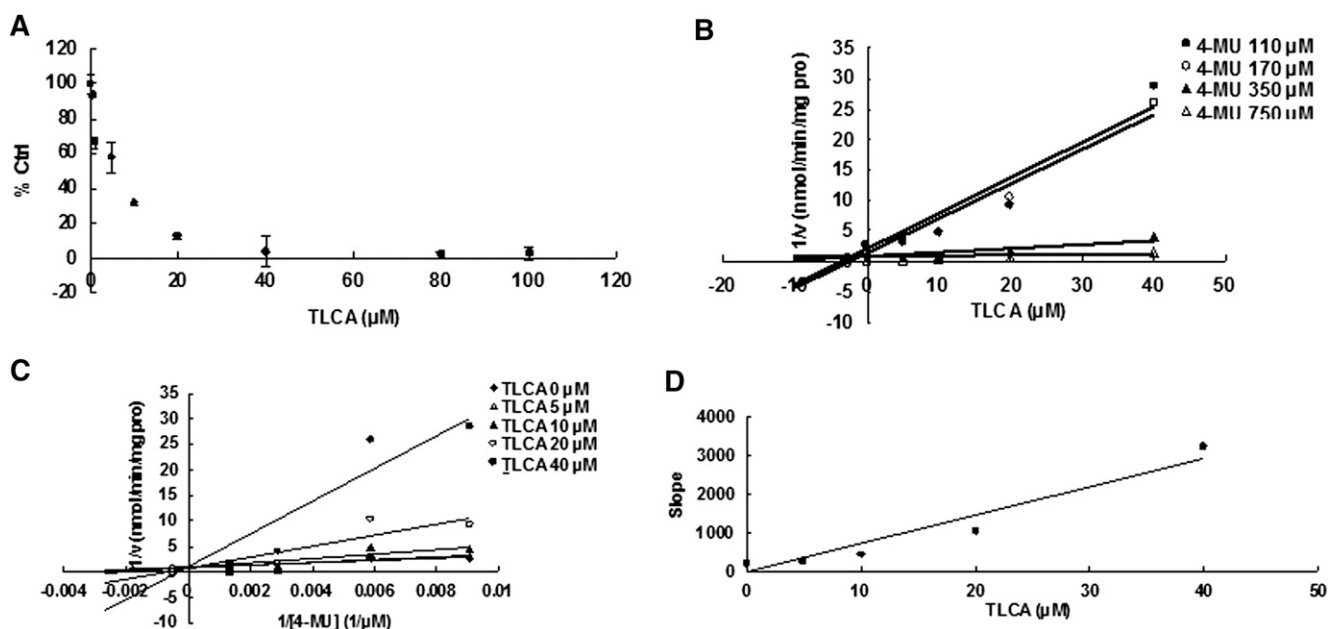
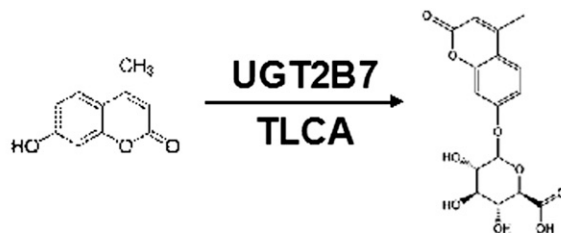


Fig. 7. Evaluation of TLCA's inhibition toward recombinant UGT2B7-catalyzed 4-MU glucuronidation. **A:** TLCA exhibited concentration-dependent inhibition toward recombinant UGT2B7-catalyzed 4-MU glucuronidation. **B:** Dixon plot of TLCA's inhibition toward recombinant UGT2B7-catalyzed 4-MU glucuronidation. **C:** Lineweaver-Burk plot of TLCA's inhibition toward recombinant UGT2B7-catalyzed 4-MU glucuronidation. **D:** Second plot of TLCA's inhibition toward recombinant UGT2B7-catalyzed 4-MU glucuronidation. The data point represents the mean of the duplicate experiments.

DISCUSSION

The inhibitory capability of BAs toward UGTs is difficult to study using conventional animal models due to the complexity of factors influencing activity *in vivo*. For example, the role of BA in the activation of nuclear receptors might interfere with the evaluation of BA inhibition toward UGT enzymes. The pregnane X receptor was found to be activated by LCA (18, 19). LCA can also activate the vitamin D receptor (20). CDCA, CA, GCA, and GCDCA were reported to be agonists of farnesoid X receptor (FXR) (21–23). Tauro- β -muricholic acid in mice was reported to be a naturally occurring FXR antagonist (24). All affected nuclear receptors regulate the expression and activity of different genes encoding UGT enzymes. For example, BAs can induce the activity of UGT2B4 via activation of FXR (25). The UGT2B4 promoter also contains a peroxisome proliferator-activated receptor (PPAR) α response element, and can be activated by PPAR α agonist fenofibrate (26). The activity of UGT2B7 can be inhibited by hydrophobic BAs via a negative FXR response element located in the UGT2B7 promoter (27). FXR activation can also regulate the expression of UGT1A3 (28). To avoid these complex factors, a relatively simple *in vitro* UGT enzyme incubation system was utilized in the present study.

The detailed metabolic inhibition profile of BAs toward important UGT isoforms was clarified in the present study, and TLCA was demonstrated to be the strongest inhibitor toward most of UGT isoforms, followed by LCA, which is consistent with the reports in which LCA and TLCA were reported to be able to significantly induce the liver damage (29, 30). LCA can be metabolized through UGT isoform-catalyzed glucuronidation elimination, so, the wide inhibition of LCA toward UGT isoforms was observed in the present study. TLCA has similar structure with LCA, and can enter the activity cavity. However, TLCA cannot be metabolized through glucuronidation by our present study (data not shown). Therefore, TLCA exhibited stronger inhibition than LCA. CA and GCA, at 100 μ M, were found to increase the activity of UGT1A3 by 35 and 45%, respectively. Given that induced expression of UGT1A3 through nuclear receptors does not occur in the present *in vitro* system, the allosteric activation of CA and GCA toward UGT1A3 might be the potential reason. However, the detailed mechanism needs to be further investigated.

According to the predicted values of AUC_i/AUC , TLCA exhibited the strongest inhibition toward UGT1A4-catalyzed metabolic reaction. UGT1A4 is widely accepted to be

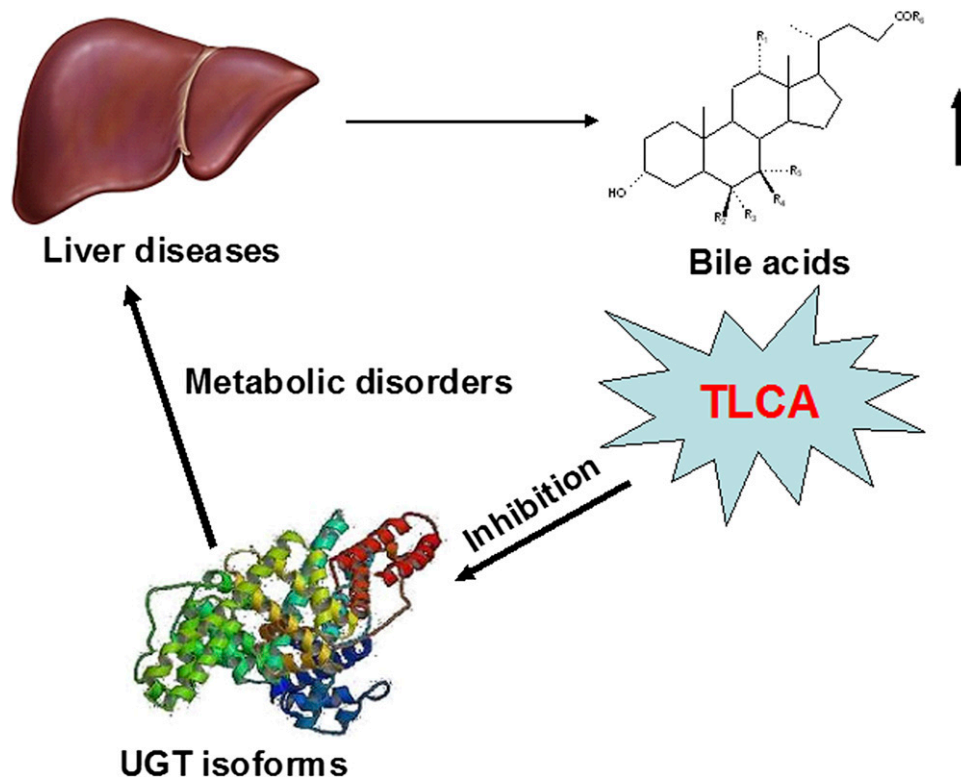


Fig. 9. Brief summary of the influence of elevated BAs toward hepatic metabolism of xenobiotics and endobiotics.

The disrupted homeostasis of BAs due to diseases (e.g., cholestasis) could inhibit UGT-catalyzed metabolism resulting in altered metabolism of xenobiotics and endogenous compounds.^[11]

REFERENCES

1. Yang, L., A. Xiong, Y. He, Z. Wang, C. Wang, Z. Wang, W. Li, L. Yang, and Z. Hu. 2008. Bile acids metabolomic study on the CCl₄- and α -naphthylisothiocyanate-induced animal models: quantitative analysis of 22 bile acids by ultraperformance liquid chromatography-mass spectrometry. *Chem. Res. Toxicol.* **21**: 2280–2288.
2. Russell, D. W. 2003. The enzymes, regulation, and genetics of bile acid synthesis. *Annu. Rev. Biochem.* **72**: 137–174.
3. Elliott, W. H., and P. M. Hyde. 1971. Metabolic pathways of bile acid synthesis. *Am. J. Med.* **51**: 568–579.
4. Palmeira, C. M., and A. P. Rolo. 2004. Mitochondrially-mediated toxicity of bile acids. *Toxicology.* **203**: 1–15.
5. Kiang, T. K., M. H. Ensom, and T. K. Chang. 2005. UDP-glucuronosyltransferases and clinical drug-drug interactions. *Pharmacol. Ther.* **106**: 97–132.
6. Matern, H., S. Matern, C. Schelzig, and W. Gerok. 1980. Bile acid UDP-glucuronosyltransferase from human liver. Properties and studies on aglycone substrate specificity. *FEBS Lett.* **118**: 251–254.
7. Parquet, M., M. Pessah, E. Sacquet, C. Salvat, A. Raizman, and R. Infante. 1985. Glucuronidation of bile acids in human liver, intestine and kidney. An in vitro study on hyodeoxycholic acid. *FEBS Lett.* **189**: 183–187.
8. Trottier, J., M. Verreault, S. Grepper, D. Monte, J. Belanger, J. Kaeding, P. Caron, T. T. Inaba, and O. Barbier. 2006. Human UDP-glucuronosyltransferase (UGT)1A3 enzyme conjugates chenodeoxycholic acid in the liver. *Hepatology.* **44**: 1158–1170.
9. Gall, W. E., G. Zawada, B. Mojarrabi, T. R. Tephly, M. D. Green, B. L. Coffman, P. I. Mackenzie, and A. Radominska-Pandya. 1999. Differential glucuronidation of bile acids, androgens and estrogens by human UGT1A3 and 2B7. *J. Steroid Biochem. Mol. Biol.* **70**: 101–108.
10. Pillot, T., M. Ouzzine, S. Fournel-Gigleux, C. Lafaurie, A. Radominska, B. Burchell, G. Siest, and J. Magdalou. 1993. Glucuronidation of hyodeoxycholic acid in human liver. Evidence for a selective role of UDP-glucuronosyltransferase 2B4. *J. Biol. Chem.* **268**: 25636–25642.
11. Schneider, H., H. Fiander, R. K. Latta, and N. W. Ross. 1993. Bile acid inhibition of xenobiotic-metabolizing enzymes is a factor in the mechanism of colon carcinogenesis: tests of aspects of the concept with glucuronosyltransferase. *Eur. J. Cancer Prev.* **2**: 393–400.
12. Fang, Z. Z., Y. F. Cao, C. M. Hu, M. Hong, X. Y. Sun, G. B. Ge, Y. Liu, Y. Y. Zhang, L. Yang, and H. Z. Sun. 2013. Structure-inhibition relationship of ginsenosides towards UDP-glucuronosyltransferases (UGTs). *Toxicol. Appl. Pharmacol.* **267**: 149–154.
13. Lu, H., Z. Z. Fang, Y. F. Cao, C. M. Hu, M. Hong, X. Y. Sun, H. Li, Y. Liu, X. Fu, and H. Sun. 2013. Isoliquiritigenin showed strong inhibitory effects towards multiple UDP-glucuronosyltransferase (UGT) isoform-catalyzed 4-methylumbelliferone (4-MU) glucuronidation. *Fitoterapia.* **84**: 208–212.
14. Uchaipichat, V., P. I. Mackenzie, D. J. Elliot, and J. O. Miners. 2006. Selectivity of substrate (trifluoperazine) and inhibitor (amitriptyline, androsterone, canrenoic acid, hecogenin, phenylbutazone, quinidine, quinine, and sulfinpyrazone) “probes” for human UDPglucuronosyltransferases. *Drug Metab. Dispos.* **34**: 449–456.
15. Tanaka, N., T. Matsubara, K. W. Krausz, A. D. Patterson, and F. J. Gonzalez. 2012. Disruption of phospholipid and bile acid homeostasis in mice with nonalcoholic steatohepatitis. *Hepatology.* **56**: 118–129.
16. Abu-Hayeh, S., G. Papacleovoulou, A. Lovgren-Sandblom, M. Tahir, O. Oduwole, N. A. Jamaludin, S. Ravat, V. Nikolova, J. Chambers, C. Selden, et al. 2013. Intrahepatic cholestasis of pregnancy levels of sulfated progesterone metabolites inhibit farnesoid X receptor resulting in a cholestatic phenotype. *Hepatology.* **57**: 716–726.
17. Takikawa, H., T. Maruyama, S. Ota, K. Matsumoto, T. Suqimoto, and E. Takano. 1984. Conjugated hyperbilirubinemia in an autopsy case with myocardial infarction and sepsis. *Jpn. J. Med.* **23**: 258–260.
18. Staudinger, J. L., B. Goodwin, S. A. Jones, D. Hawkins-Brown, K. I. MacKenzie, A. LaTour, Y. Liu, C. D. Klaassen, K. K. Brown, J.

- Reinhard, et al. 2001. The nuclear receptor PXR is a lithocholic acid sensor that protects against liver toxicity. *Proc. Natl. Acad. Sci. USA*. **98**: 3369–3374.
19. Xie, W., A. Radominska-Pandya, Y. Shi, C. M. Simon, M. C. Nelson, E. S. Ong, D. J. Waxman, and R. M. Evans. 2001. An essential role for nuclear receptors SXR/PXR in detoxification of cholestatic bile acids. *Proc. Natl. Acad. Sci. USA*. **98**: 3375–3380.
20. Makishima, M., T. T. Lu, W. Xie, G. K. Whitfield, H. Domoto, R. M. Evans, M. R. Haussler, and D. J. Mangelsdorf. 2002. Vitamin D receptor as an intestinal bile acid sensor. *Science*. **296**: 1313–1316.
21. Fujino, T., M. Une, T. Imanaka, K. Inoue, and T. Nishimaki-Mogami. 2004. Structure-activity relationship of bile acids and bile acid analogs in regard to FXR activation. *J. Lipid Res.* **45**: 132–138.
22. Parks, D. J., S. G. Blanchard, R. K. Bledsoe, G. Chandra, T. G. Consler, S. A. Kliewer, J. B. Stimmel, T. M. Willson, A. M. Zavacki, D. D. Moore, et al. 1999. Bile acids: natural ligands for an orphan nuclear receptor. *Science*. **284**: 1365–1368.
23. Nakahara, M., N. Furuya, K. Takagaki, T. Sugaya, K. Hirota, A. Fukamizu, T. Kanda, H. Fujii, and R. Sato. 2005. Ileal bile acid-binding protein, functionally associated with the farnesoid X receptor or the ileal bile acid transporter, regulates bile acid activity in the small intestine. *J. Biol. Chem.* **280**: 42283–42289.
24. Li, F., C. Jiang, K. W. Krausz, Y. Li, I. Albert, H. Hao, K. M. Fabre, J. B. Mitchell, A. D. Patterson, and F. J. Gonzalez. 2013. Microbiome remodelling leads to inhibition of intestinal farnesoid X receptor signalling and decreased obesity. *Nat. Commun.* **4**: 2384.
25. Barbier, O., I. P. Torra, A. Sirvent, T. Claudel, C. Blanquart, D. Duran-Sandoval, F. Kuipers, V. Kosykh, J. C. Fruchart, and B. Staels. 2003. FXR induces the UGT2B4 enzyme in hepatocytes: a potential mechanism of negative feedback control of FXR activity. *Gastroenterology*. **124**: 1926–1940.
26. Barbier, O., D. Duran-Sandoval, I. Pineda-Torra, V. Kosykh, J. C. Fruchart, and B. Staels. 2003. Peroxisome proliferator-activated receptor alpha induces hepatic expression of the human bile acid glucuronidating UDP-glucuronosyltransferase 2B4 enzyme. *J. Biol. Chem.* **278**: 32852–32860.
27. Lu, Y., J. M. Heydel, X. Li, S. Bratton, T. Lindblom, and A. Radominska-Pandya. 2005. Lithocholic acid decreases expression of ugt2b7 in Caco-2 cells: a potential role for a negative farnesoid X receptor response element. *Drug Metab. Dispos.* **33**: 937–946.
28. Erichsen, T. J., A. Aehlen, U. Ehmer, S. Kalthoff, M. P. Manns, and C. P. Strassburg. 2010. Regulation of the human bile acid UDP-glucuronosyltransferase 1A3 by the farnesoid X receptor and bile acids. *J. Hepatol.* **52**: 570–578.
29. Matsubara, T., N. Tanaka, M. Sato, D. W. Kang, K. W. Krausz, K. C. Flanders, K. Ikeda, H. Luecke, L. M. Wakefield, and F. J. Gonzalez. 2012. TGF- β -SMAD3 signaling mediates hepatic bile acid and phospholipid metabolism following lithocholic acid-induced liver injury. *J. Lipid Res.* **53**: 2698–2707.
30. Mottino, A., B. Tuchweber, G. L. Plaa, and I. M. Yousef. 2000. Role of perivenous hepatocytes in taurolithocholate-induced cholestasis in vivo. *Toxicol. Lett.* **116**: 69–77.
31. Kuehl, G. E., and S. E. Murphy. 2003. N-glucuronidation of nicotine and cotinine by human liver microsomes and heterologously expressed UDP-glucuronosyltransferases. *Drug Metab. Dispos.* **31**: 1361–1368.
32. Modica, S., S. Murzilli, L. Salvatore, D. R. Schmidt, and A. Moschetta. 2008. Nuclear bile acid receptor FXR protects against intestinal tumorigenesis. *Cancer Res.* **68**: 9589–9594.
33. Butler, L. M., Y. Duguay, R. C. Millikan, R. Sinha, J. F. Gagne, R. S. Sandler, and C. Guillemette. 2005. Joint effects between UDP-glucuronosyltransferase 1A7 genotype and dietary carcinogen exposure on risk of colon cancer. *Cancer Epidemiol. Biomarkers Prev.* **14**: 1626–1632.
34. Dellinger, R. W., G. Chen, A. S. Blevins-Primeau, J. Krzeminski, S. Amin, and P. Lazarus. 2007. Glucuronidation of PhIP and N-OH-PhIP by UDP-glucuronosyltransferase 1A10. *Carcinogenesis*. **28**: 2412–2418.